Nuclear Physics B121 (1977) 31–37

SMALL-ANGLE COMPTON SCATTERING ON HYDROGEN AND DEUTERIUM

L. CRIEGEE, G. FRANKE, A. GIESE, Th. KAHL, G. POELZ, U. TIMM, H. WERNER and W. ZIMMERMANN
Deutsches Elektronen-Synchrotron DESY, Hamburg, Germany

Received 6 December 1976

We have measured elastic scattering of 5 and 6 GeV photons on hydrogen and deuterium in the angular range 10–50 mrad. On hydrogen we observe a forward diffraction peak with a slope of 8.5 $(\mathrm{GeV}/c)^{-2}$. The extrapolated forward cross sections in units $\mu\mathrm{b}/(\mathrm{GeV}/c)^2$ are 0.82 ± 0.04 at 5 GeV and 0.79 ± 0.04 at 6 GeV. They are consistent with the calculated amplitudes obtained from total cross section measurements *via* the optical theorem and dispersion relations assuming negligible contributions of spin-dependent amplitudes. Deuterium cross sections show a transition from coherent scattering at low $|t|$ to incoherent scattering at higher $|t|$. They indicate that the isovector exchange amplitude a_1 is very small compared to the isoscalar a_0. We obtain

$$|a_1|^2/|a_0 + a_1|^2 = 0.13 \pm 0.09 ,$$

$$\mathrm{Re}(a_0 a_1^*)/|a_0 + a_1|^2 = 0.0 \pm 0.03 , \quad \text{at 5 GeV} ,$$

$$|a_1|^2/|a_0 + a_1|^2 = -0.12 \pm 0.15 ,$$

$$\mathrm{Re}(a_0 a_1^*)/|a_0 + a_1|^2 = 0.10 \pm 0.04 , \quad \text{at 6 GeV} .$$

Many conclusions drawn from elastic photon-nucleon scattering depend on a precise knowledge of the forward cross section. Photon detectors trying to approach the forward direction, however, have to cope with an increasing background caused by QED reactions. We have measured Compton scattering on hydrogen and deuterium at 6 GeV, and in a second, slightly modified experiment at 5 GeV, both at particularly small momentum transfers ranging from –0.004 to –0.08 $(\mathrm{GeV}/c)^2$ at 6 GeV and from –0.002 to –0.06 $(\mathrm{GeV}/c)^2$ at 5 GeV.

The experimental setup is shown schematically in fig. 1. A bremsstrahlung beam from the DESY synchrotron hits a target of liquid H_2 (or D_2), 20 cm long. Since the energy of the recoiling nuclei is too small to be measured, only the scattered photons are registered. Photon energy and angles are measured in a pair spectrometer consisting of a 4 mm thick Al converter, one bending magnet and two telescopes

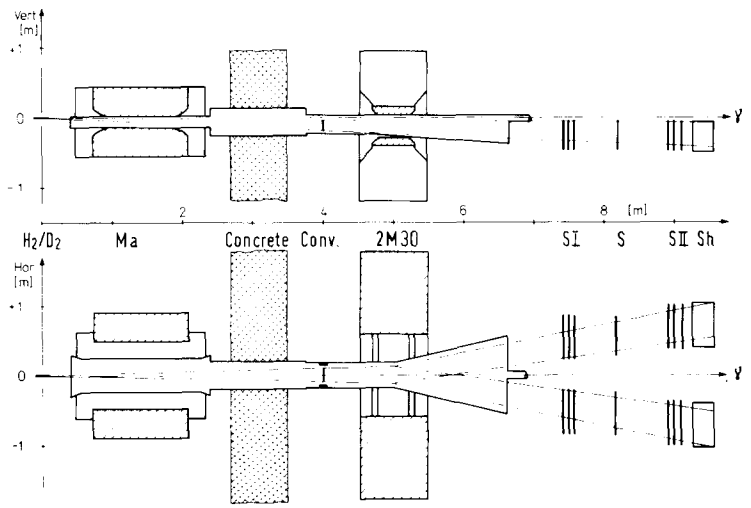

Fig. 1. Schematic view of the magnetic Compton spectrometer. Side view and top view. H_2/D_2: Target; Ma: Cleaning magnet; Conv: Converter; 2M30: Analyzing magnet; SI, S, SII: Spark chambers; Sh: Shower counters.

equipped with 7 spark chambers and one shower counter each. The energy resolution of the spectrometer was 1.3% (FWHM).

Special care was taken to prepare the incoming photon beam so that it produced little halo at the converter position: The beam originated in a small (2×2 mm^2) source and was shaped and cleaned by three collimators with subsequent clearing magnets. It was guided through vacuum whereever possible. The empty target rate varied between 2% and 25%, depending on the scattering angle. No events were recorded when the converter was removed.

The beam intensity and spectrum were continuously measured by a second pair spectrometer, placed downstream in the main beam. The intensity was also monitored by a thick-walled ionization chamber (quantameter). It was corrected for absorption between the experiment and the monitors. The systematic error of the intensity is ±1.2%.

Photons from electron Compton scattering were eliminated by their energy being less than 80% of the maximum beam energy in the angular interval covered by the converter. Accidental and multiple track rates caused by this and other sources of background were lower than 1.2%.

The contribution of inelastic hadronic reactions were separated by means of the different photon spectra they produce. The energy spectrum of Compton scattered photons reproduces the sharp edge of the primary beam spectrum while the spectra of inelastic processes vanish smoothly at the end point. Fig. 2 demonstrates the different shapes.

Both Compton scattering and inelastic reactions were simulated by Monte Carlo

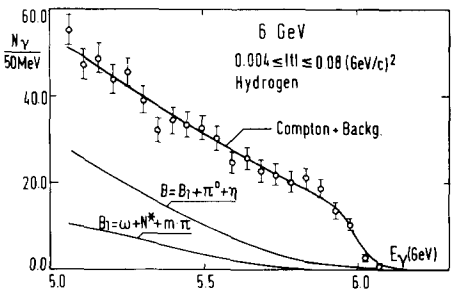

Fig. 2. Reconstructed spectrum of photons scattered on protons at 6 GeV with $0.004 \leqslant |t| \leqslant 0.08$ $(\mathrm{GeV}/c)^2$. Also shown is the result of a fit separating Compton- and background contributions.

calculations as a function of the photon energy k and the four-ommentum transfer $|t|$.

Inelastic reactions considered are the reactions $\gamma p \to \pi^0 p$ with $\pi^0 \to \gamma\gamma$ and $\gamma p \to \eta p$ with $\eta \to \gamma\gamma$ [1,2]. They lead to a spectrum known to about 20% accuracy, which will be called B2 thereafter. Further background contributions result from the reactions $\gamma p \to \gamma N^*$ with N*(1470), N*(1520) and N*(1688) [3], the processes $\gamma p \to \omega p$ with $\omega \to \gamma\pi^0$ [4], and multipion production $\gamma p \to \gamma p + m\pi$ with $m \geqslant 1$ [3], giving a spectrum referred to as B1 below. The sum of the Compton spectrum, B1 and B2 was then fitted to the measured spectrum, with the magnitudes of the Compton spectrum, of B1, and the end energy as free parameters. For obtaining the t-dependence, the end energy was then kept fixed, and the spectra were fitted for each t-bin separately.

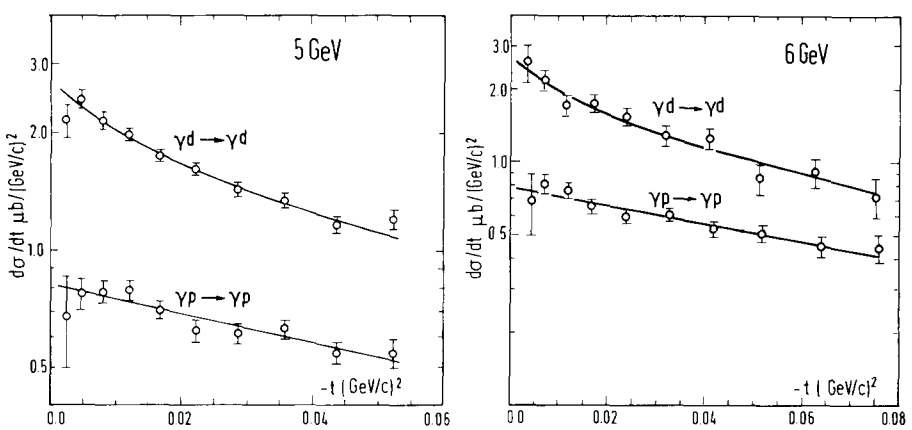

Fig. 3. Differential cross sections for Compton scattering on hydrogen and deuterium at 5 and 6 GeV. Also shown is the result of an exponential fit to the hydrogen data, and of a form factor fit to the deuteron data, see text.

Table 1
Differential Compton cross section for hydrogen and deuterium at 5 GeV and 6 GeV (also shown is the Glauber correction parametrized as $G(t) = 1 - X(t)$, calculated from the deuteron wave function following Reid [15])

5 GeV	Hydrogen		Deuterium		
$-t$ $(\mathrm{GeV}/c)^2$	$d\sigma/dt$ (H) $\mu b(\mathrm{GeV}/c)^2$	stat. error	$d\sigma/dt$ (D) $\mu b/(\mathrm{GeV}/c)^2$	stat. error	$X(t)$
0.0016–0.0036	0.68	±0.14	2.16	±0.21	0.055
0.0036–0.0064	0.78	±0.07	2.42	±0.10	0.058
0.0064–0.0100	0.78	±0.05	2.15	±0.08	0.062
0.0100–0.0144	0.79	±0.04	1.99	±0.06	0.066
0.0144–0.0196	0.70	±0.04	1.75	±0.05	0.069
0.0196–0.0256	0.62	±0.04	1.62	±0.05	0.073
0.0256–0.0324	0.61	±0.03	1.43	±0.05	0.077
0.0324–0.0400	0.63	±0.03	1.35	±0.05	0.080
0.0400–0.0484	0.55	±0.03	1.17	±0.05	0.084
0.0484–0.0576	0.54	±0.04	1.20	±0.07	0.087

6 GeV	Hydrogen		Deuterium		
$-t$ $(\mathrm{GeV}/c)^2$	$d\sigma/dt$ $\mu b/(\mathrm{GeV}/c)^2$	stat. error	$d\sigma/dt$ (D) $\mu b/(\mathrm{GeV}/c)^2$	stat. error	$X(t)$
0.0040–0.0052	0.69	±0.17	2.56	±0.39	0.063
0.0052–0.0092	0.81	±0.06	2.17	±0.14	0.067
0.0092–0.014	0.77	±0.05	1.71	±0.10	0.071
0.014 –0.021	0.66	±0.04	1.74	±0.08	0.076
0.021 –0.028	0.60	±0.03	1.54	±0.07	0.081
0.028 –0.037	0.61	±0.03	1.28	±0.06	0.085
0.037 –0.047	0.53	±0.03	1.25	±0.06	0.088
0.047 –0.058	0.51	±0.03	0.86	±0.05	0.092
0.058 –0.070	0.45	±0.03	0.91	±0.05	0.096
0.070 –0.083	0.45	±0.04	0.72	±0.06	0.100

The differential cross sections determined in this way are listed in table 1 and shown in fig. 3. Only statistical errors are shown. Systematic errors result mainly from the uncertainty of the background B2 (±1%) of the converter position (1.5%), and in the case of the 6 GeV data from the error in the telescope efficiencies (1.5%). By quadratic addition to the normalization error we obtain a total systematic error of 2.5% at 5 GeV and 3.6% at 6 GeV.

A fit to our data of the form $d\sigma/dt = A \exp(Bt)$, as suggested by diffraction theory, yields the results shown in table 2 (see curves in fig. 3). The errors include statistical errors as well as the total systematic error.

The extrapolated forward cross sections are shown in fig. 4 as a function of the

Table 2
Parameters of an exponential fit to the Compton cross section on hydrogen of the form $d\sigma/dt = A \exp(Bt)$

	Photon energy (GeV)	$d\sigma/dt$ (0) $\mu b/(GeV/c)^2$	B $(GeV/c)^{-2}$
This experiment	5	0.82 ± 0.04	8.5 ± 1.5
	6	0.79 ± 0.04	8.6 ± 1.2
DESY [5]	4–6.2	0.84 ± 0.08	5.7 ± 0.35
SLAC [7]	8	0.82 ± 0.04	7.7 ± 0.5
VDM prediction	5	0.46 ± 0.05	
(see text)	6	0.44 ± 0.04	

laboratory photon energy. They agree with earlier coincidence measurements in the same energy region [5–7]. For comparison, the solid curve shows the forward cross section as derived from total cross section measurements *via* the optical theorem and dispersion relations [8], assuming the spin-dependent amplitude to be zero. This predicted cross section is about 10% higher than the new and some of the earlier measurements. Whether this difference is due to systematic errors in the underlying measurements, or to a failure of the straight-line extrapolation at very small angles, is unknown to us. The sign of the difference certainly argues against a sizeable contribution of the spin-dependent amplitude, since it would add to the prediction.

For comparison with the predictions of the vector dominance model, VDM, the

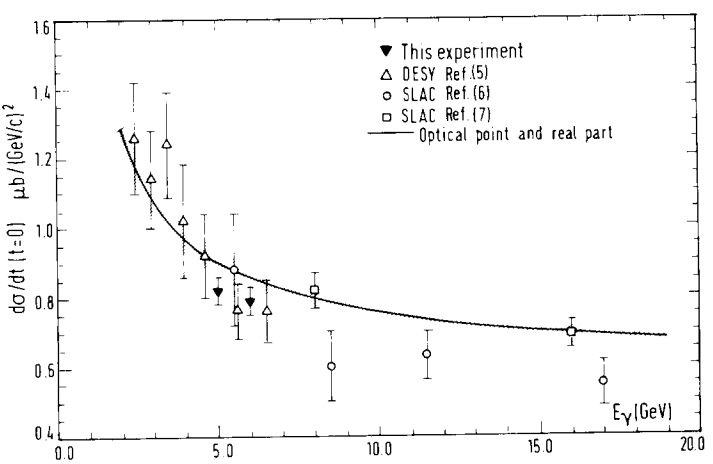

Fig. 4. Forward Compton cross sections on hydrogen *versus* photon energy. Also shown is the expected value as calculated from the optical theorem including a real part [8]; the shaded area indicates the error of about 4% in $\sigma_{tot}(\gamma p)$ [16].

Table 3
Isospin ratios in the photon-nucleon interaction

		$\frac{\lvert a_1\rvert^2}{\lvert a_0+a_1\rvert^2}$	$\frac{\mathrm{Re}(a_0 a_1^*)}{\lvert a_0+a_1\rvert^2}$
This experiment	5 GeV	0.13 ± 0.09	0. ± 0.03
		(0.08 ± 0.10	0.02 ± 0.03)*
	6 GeV	−0.12 ± 0.15	0.10 ± 0.04
		(−0.12 ± 0.15	0.10 ± 0.04)*
SLAC [7]	8 and 16 GeV	0.03 ± 0.10	−0.043 ± 0.012
		(0.02 ± 0.12	0.02 ± 0.02)**
This experiment and SLAC [7]		0.08 ± 0.05	0.02 ± 0.01
DESY [16]		$\frac{\mathrm{Im}\, a_1}{\mathrm{Im}\, a_0} = 0.042 \pm 0.008$	

The analysis of this experiment uses a deuteron wave function following Reid. For comparison, a calculation with Hulthén wave functions (*) is shown, and also an analysis of the data from ref. [7] using Reid's wave function (**).

foreward cross sections have been calculated using the sum rule

$$\frac{\mathrm{d}\sigma}{\mathrm{d}t}(\gamma p \to \gamma p) = \left[\sum_V \left(\tfrac{1}{4}\alpha \frac{4\pi}{\gamma_V^2} \frac{\mathrm{d}\sigma}{\mathrm{d}t}(\gamma p \to V p)\right)^{1/2}\right]^2 ,$$

with recent values for the vector meson cross sections [9] and the Orsay values for the coupling constants $\frac{1}{4}\alpha\, 4\pi/\gamma_V^2$ [10]. Table 2 demonstrates the well known discrepancy: The data are higher by about 40% than the VDM predictions. This discrepancy can be removed by including the higher vector mesons $\rho'(1600)$, $\psi(3100)$ and $\psi'(3700)$ and by extending the VDM to the GVDM [11].

The differential cross section for the deuteron (figs. 3a, b) shows the transition from coherent scattering at low $|t|$ to incoherent scattering at higher $|t|$ values. Neglecting spin effects the cross section can be written in closure approximation as

$$\left.\frac{\mathrm{d}\sigma}{\mathrm{d}t}\right|_{\mathrm{d}} = \frac{2\pi}{k^2}\left[\lvert a_0\rvert^2(1+F(t)) + \lvert a_1\rvert^2(1-F(t))\right] G(t) ,$$

where k is the photon energy. $F(t)$ and $G(t)$ denote the deuteron form factor and the Glauber correction factor [12]. a_0 and a_1 are the amplitudes of isospin 0 and 1 exchange. The influence of the Fermi motion [13] is smaller than the Glauber correction, according to our own calculations. The corresponding differential proton cross section is given by

$$\left.\frac{\mathrm{d}\sigma}{\mathrm{d}t}\right|_{\mathrm{p}} = \frac{\pi}{k^2}\left(\lvert a_0\rvert^2 + \lvert a_1\rvert^2 + 2\,\mathrm{Re}(a_0 a_1^*)\right) .$$

From the deuteron and the proton cross sections one can deduce the two isospin ratios $|a_1|^2/|a_0 + a_1|^2$ and $\mathrm{Re}(a_0 a_1^*)/|a_0 + a_1|^2$. By a fit to our experimental data (also shown in fig. 3) we obtain the values listed in table 3. Systematic errors resulting mainly from the uncertainty in the B2 background component and in the precise converter position, amount to about half of the statistical errors, while normalization errors common to both targets should have no effect.

The isospin ratios depend however sensitively on the assumed shape of $F(t)$ and $G(t)$. We have used a deuteron wave function following Reid [14] and calculated $G(t)$ in the ρ-dominance approximation. If we analyse the data starting from a Hulthén wave function [15], we obtain consistent, although numerically different ratios. For comparison we have also calculated these parameters from the data of Boyarski et al. [7] using our Glauber corrections. The values are then changed slightly as shown in table 3.

All the ratios are compatible with a vanishing or at least small isospin 1 exchange contribution to photon nucleon interaction. They are also compatible with the measured [16] ratio

$$\frac{\mathrm{Im}\, a_1}{\mathrm{Im}\, a_0} = \frac{\sigma(\gamma p) - \sigma(\gamma n)}{\sigma(\gamma p) + \sigma(\gamma n)} ,$$

as listed in table 3, if one assumes equal real and imaginary parts of the a_1 amplitude as predicted for A_2 Regge exchange.

References

[1] M. Braunschweig et al., Nucl. Phys. B20 (1970) 191 and private communication.
[2] W. Braunschweig et al., Phys. Letters 33B (1970) 236.
[3] G. Wolf, Nucl. Phys. B26 (1971) 317.
[4] Y. Eisenberg et al., Phys. Letters 34B (1971) 439.
[5] G. Buschhorn et al., Phys. Letters 37B (1971) 207.
[6] R.L. Anderson et al., Phys. Rev. Letters 25 (1970) 1218.
[7] A.M. Boyarski et al., Phys. Rev. Letters 26 (1971) 1600; 30 (1973) 1098.
[8] M. Damashek and F.J. Gilman, Phys. Rev. D1 (1970) 1319.
[9] J. Ballam et al., Phys. Rev. D7 (1973) 3150.
[10] J. Perez-Y-Jorba, in Proc. 4th Int. Symp. on electron and photon interactions at high energies, Liverpool, 1970.
[11] J.J. Sakurai and D. Schildknecht, Phys. Letters 42B (1972) 216 and references therein.
[12] V. Franco and R.J. Glauber, Phys. Rev. 142 (1966) 1195.
[13] W.B. Atwood and G.B. West, Phys. Rev. D7 (1973) 773;
A. Bodek, Phys. Rev. D8 (1973) 2331.
[14] R.V. Reid, Ann. of Phys. 50 (1968) 411.
[15] G.F. Chew and H.W. Lewis, Phys. Rev. 84 (1951) 779.
[16] G. Wolf, Proc. 5th Int. Symp. on electron and photon interactions at high energies, Cornell University, 1971.